Aerosol and Air Quality Research, 19: 2557–2567, 2019

ISSN: 1680-8584 print / 2071-1409 online
doi: 10.4209/aaqr.2019.09.0468

Using Rice-husk-derived Porous Silica Modified with Recycled Cu from Industrial Wastewater and Ce to Remove Hg^0 and NO from Simulated Flue Gases

Ming-Yin Chen[1], Yun-Chih Tsai[2], Chih-Fu Tseng[1,3], Hong-Ping Lin[2*], Hsing-Cheng Hsi[1*]

[1] *Graduate Institute of Environmental Engineering, National Taiwan University, Taipei 10617, Taiwan*
[2] *Department of Chemistry, National Cheng-Kung University, Tainan 70101, Taiwan*
[3] *Taiwan Power Research Institute, Taiwan Power Company, New Taipei City 23847, Taiwan*

ABSTRACT

Resource-recovered CuO_x-CeO_x/SiO_2 samples were prepared by using rice-husk-derived silica modified with recycled copper ion from panel industry wastewater for controlling Hg^0 and NO emissions from simulated flue gases. By using the silicate exfoliation method for sample preparation, the presence of Cu and Ce oxides could increase the specific surface area (S_{BET}) of SiO_2. 50%Cu-10%Ce/SiO_2 having the largest S_{BET} showed significant NO removal. XRD results indicated that significant CuO diffraction peaks were not detected among all the CuO_x/SiO_2 samples, suggesting that CuO_x was highly dispersed on the surface. SEM and TEM images showed that the uniform spherical SiO_2 particles have changed into plate-like structure, further confirming the occurrence of structural rearrangement after incorporated with Cu/Ce oxides via silicate exfoliation. XPS results showed that Cu^{2+} and Ce^{4+} were the major valence states presenting in the samples. H_2-TPR and NH_3-TPD indicated that the 50%Cu/SiO_2 and 50%Cu-10%Ce/SiO_2 had greater redox ability and stronger acidity as compared to those containing smaller amounts of CuO_x and CeO_x. Cu and Ce modification was shown to successfully improve the NO removal efficiency. 50%Cu-10%Ce/SiO_2 had the best NO conversion efficiency of 70–85% with a broad temperature window of 150–300°C. 50%Cu/SiO_2 exhibited the greatest total Hg removal efficiency of 88.2% among all the tested samples at 150°C and remained almost the same removal efficiency at 250°C. These results suggest that the recycled Cu modified rice-husk-derived SiO_2 is feasible for not only controlling Hg^0 and NO emissions but also recovery of agricultural and industrial wastes.

Keywords: Mercury; NO_x; Copper oxides; Rice-husk-derived silica; Silicate exfoliation.

INTRODUCTION

Mercury (Hg) and NO_x discharged from coal-fired power plants (CFPPs) have both received special concern owing to the high toxicity and long retention time in the environment of Hg and the formation of acid rain, photocatalytic smog and secondary $PM_{2.5}$ from NO_x (Gao *et al.*, 2017; Zhang *et al.*, 2017; UNEP, 2018; U.S. EPA, 2019). Hg^0 has been known hardly removed due to its high stability and volatility as compared to Hg^{2+} and particulate Hg (Hg_p). Instead of using activated carbon to capture Hg^0 (Chou *et al.*, 2018), catalytic transformation of Hg^0 to Hg^{2+} and subsequently to Hg_p by metal-oxide selective catalytic reduction (SCR) catalysts is beneficial, not only the formed Hg^{2+} and Hg_p can be removed by downstream flue gas desulfurization device(FGD) but also NO_x reduction could be simultaneously achieved. Catalytic oxidation of Hg^0 using different metal-oxide catalysts in CFPP gases has been examined (Wang *et al.*, 2013, 2014; Xiong *et al.*, 2017). Numerous studies have also been conducted to comprehend the simultaneous removal of Hg^0 and NO (Li *et al.*, 2011; He *et al.*, 2013; Chang *et al.*, 2015; Li *et al.*, 2015; Zhao *et al.*, 2016; Song *et al.*, 2018; Lin *et al.*, 2019). The influencing factors on the removal effectiveness of Hg^0 and NO_x include flue gas composition and temperature, the physiochemical characteristics of catalysts, and the dosage of NH_3 for NO_x reduction that could limit Hg^0 removal by competing the adsorption sites.

A summary of selected research on novel metal oxides for Hg^0 and NO removal is listed in Table S1. Although V_2O_5-WO_3/TiO_2 and V_2O_5-MoO_3/TiO_2 are the most widely applied industrial catalysts for the SCR process, several kinds of transitional metal oxides, including CuO_x and CeO_2, are also active for NH_3-SCR reactions and have attracted great attention in these years (Chen *et al.*, 2014; Chiu *et al.*, 2015; Chen *et al.*, 2018; Fan *et al.*, 2018; Jiang *et al.*, 2018; Liu *et al.*, 2018). Sullivan *et al.* (2005) indicated that two different copper precursors, $Cu(NO_3)_2$ and $CuSO_4$ impregnated on

* Corresponding author.
Tel.: +886 2 33664374; Fax: +886 2 23928830
E-mail address: hchsi@ntu.edu.tw (H.C. Hsi);
hplin@mail.ncku.edu.tw (H.P. Lin)

oxide-supported TiO_2, Al_2O_3, and SiO_2 demostrated good NH_3-SCR activity in the presence of H_2O. Chiu *et al.* (2017) reported that CuO_x/SiO_2 with high copper content (50 wt%) and large surface area/mesoporosity showed greater NO and Hg^0 removal performance as compared to VO_x and MnO_x/SiO_2. CeO_x has also received considerable attention for NH_3–SCR in recent years due to its excellent oxygen storage capacity and high redox ability via Ce^{4+} to Ce^{3+} transition (Chen *et al.*, 2014). CeO_2 mixed with other oxides, such as Mn-Ce/TiO_2, CeO_2-TiO_2, $Ce_xTi_{1-x}O_2$, CeO_2-WO_3/TiO_2, CeO_2-WO_3, and CeO_2/Al_2O_3, had great SCR activity but with poor resistance to sulfur and water poisoning (Liu *et al.*, 2012). Gao *et al.* (2010) indicated that compared with Ce-Ti (CET) oxide catalyst, the Ce-Cu-Ti (CCT) oxide catalyst showed better performance at temperatures lower than 350°C. CCT also exhibited higher SO_2-resistant ability than CET.

Mesoporous SiO_2 has been shown to successfully remove NO or Hg^0 as adsorbents or catalytic supports. Liu *et al.* (2012) reported that adding SiO_2 into TiO_2 successfully broadened the activity temperature range. The Ce/TiO_2-SiO_2 catalyst with a Ti/Si mass ratio of 3/1 exhibited the best NH_3-SCR activity and its NO_x conversion was greater than 90% at the temperature range of 250–450°C. Peng *et al.* (2013) showed that the doping of CeO_2-WO_3/TiO_2 catalyst with SiO_2 increased the reaction rate of reducing NO with NH_3 at relatively low temperatures. Zhao *et al.* (2014) indicated that SiO_2-TiO_2 nanocomposite catalyst had the greatest Hg^0 removal efficiency in the simulated flue gas when Ti: Si ratio was 2:1. Tan *et al.* (2012) also indicated the potential of Fe_2O_3-SiO_2 composite for Hg^0 removal via heterogeneous oxidation in flue gases.

Rice husk is abundantly available agricultural waste in rice-producing countries (Adam *et al.*, 2012). According to statistics from the Council of Agriculture in Taiwan, approximately six hundred thousand tons of waste rice husk were produced each year. The white ash obtained from the combustion of rice husk at moderate temperature contains 87–97% silica in an amorphous form and some amount of metallic impurities (Yalçin and Sevinç, 2001). Therefore, rice husk ash has been utilized as a silicon source to prepare high-performance products for diverse applications due to its large specific surface, high activity, and abundant silicon content (Deng *et al*., 2016).

In this research, rice-husk-derived SiO_2 incorporated with copper ion recycled from panel industrial wastewater was prepared via silicate-exfoliation method to understand the samples' removal effectiveness for Hg^0 and NO. Importantly, because the SiO_2 support and Cu ion are both recycled from wastes, the resulting materials are considered as environment-friendly catalysts and adsorbents. Furthermore, silicate-exfoliation synthesis leads to reformation of the SiO_2 surface structure, which results in uniform distribution and high loading of Cu and Ce oxides on the silica surface and high surface area and pore volume (Lin *et al*., 2019). The improvement in the abovementioned properties of materials could greatly enhance the removal of Hg^0 and NO_x, but still not yet be thoroughly comprehended.

EXPERIMENTAL SECTION

Fabrication of Metal-oxide-incorporated SiO₂ via Silicate Exfoliation

To synthesize rice-husk-derived SiO_2, 160 g of rice husk and 40 g of citric acid were first mixed in 1500 ml H_2O to hydrolyze organic matter and remove metal ions. The resulted solution was then hydrothermally treated at 100°C for 24 h. Filtration, drying, and calcination at 600°C were then employed for 6 h in air to yield the raw SiO_2 sample.

To prepare CuO_x-CeO_x/SiO_2, the weight percentages of Cu in CuO_x/SiO_2 were set at 10, 25, and 50 wt%; the weight percentages of Cu and Ce in CuO_x-CeO_x/SiO_2 were set at 50 and 10 wt%, respectively. For example, to prepare 50%Cu-10%Ce/SiO_2, 10 ml industrial wastewater with 75,000 ppm Cu and 0.51 g $Ce(NO_3)_2$ were dissolved in water to form a solution. The rice-husk-derived SiO_2 was then added into the metal salt solution. Afterward, the mixture was neutralized with 0.6 M Na_2CO_3 aqueous solution and increased pH to 9.0. After stirring for 2 h at 40°C, the resulted solution was hydrothermally treated at 100°C for 24 h. The metal oxide would incorporate with the rice-husk-derived SiO_2 during the hydrothermal process via silicate exfoliation. Filtration, drying, and calcination at 400°C were employed for 4 h in air to yield the 50%Cu-10%Ce/SiO_2 sample. The resulting metal oxide-incorporated SiO_2 was ground into powder, passed through a 50-mesh sieve, and stored for subsequent sample characterization and Hg^0 and NO removal tests.

Characterization of Metal-oxide-incorporated SiO₂

The specific surface area (S_{BET}), total pore volume (V_t), and average pore size of raw and metal-oxide-incorporated SiO_2 samples were measured by N_2 adsorption at 77K (Micromeritics ASAP-2020). Surface morphology and sample size were obtained using scanning electron microscopy (SEM; Hitachi SU8010) and transmission electron microscopy (TEM; JEOL JEM-1400). The crystalline structures of samples were examined by X-ray diffraction (XRD; Shimadzu 7000S) with Cukα radiation (λ = 1.5405 Å). The instrument was operated at 45 kV and 40 mA target current. Continuous scans were performed from 2θ = 30° to 80° with a 0.03° step size and a counting time of 4 s/step. X-ray photoelectron spectroscopy (XPS; VG Scientific ESCALAB 250) was used to examine the surface chemical compositions and valence states of metal oxides in SiO_2. For XPS examination, all binding energies were referenced to C1s peak at 285 eV. Temperature-programmed reduction of H_2 (H_2-TPR) in 10% H_2/Ar was conducted using 10 mg of sample with a total flow rate of 50 mL min^{-1}. The sample was pretreated in a pure Ar flow at 300°C for 0.5 h and cooled to 50°C before measuring the H_2-TPR. The sample was placed in dilute H_2, and the H_2 consumption was monitored using a Micromeritics Autochem 2920 by increasing the temperature to 800°C at a rate of 10°C min^{-1}. Temperature-programmed desorption of ammonia (NH_3-TPD) was also performed by a Micromeritics Autochem 2920 using 10 mg sample. The powder sample was first pretreated in 30 mL min^{-1} N_2 at 150°C for 1 h. Subsequently, the sample was cooled down to room temperature and saturated with 10% NH_3/Ar for 1 h. Adsorbed

NH_3 was removed using Ar flow (50 mL min^{-1}) for 40 min before starting the TPD experiments. After saturation, the sample was flushed in a pure Ar flow for 30 min at 100°C. Finally, the sample was heated up to 750°C with a heating rate of 10°C min^{-1}. The amount of NH_3 desorption from the samples was quantified by a thermal conductivity detector.

Hg^0/NO Removal Tests

The Hg^0 removal tests were carried out in a fixed-bed reactor with 10 mg sample using a simulated flue gas containing 30, 65, and 100 ± 5 µg m^{-3} Hg^0 at 150, 250, and 350°C. The simulated flue gas also contained 12% CO_2, 10% H_2O, 6% O_2, 50 ppm HCl, 200 ppm SO_2, 200 ppm NO, and balanced N_2 prepared from standard gas cylinders with a flow rate of 1.5 L min^{-1} at 25°C. Detailed descriptions regarding the experimental apparatus, flue gas generation, data acquisition, and removal efficiency calculation can be found in the Supplementary Material, Fig. S1, and elsewhere (Chiu *et al.*, 2015, 2017; Liu *et al.*, 2017; Lin *et al.*, 2019). Notably, the reason to test the Hg^0 removal at three different temperatures in this study was to better understand the removal dependence on flue gas temperature in coal-fired utilities, for which adsorption of Hg^0 is dominant at lower temperature and catalytic oxidation is dominant at higher temperature with presence of porous catalyst. Additionally, the flue gas temperature is typically around 150°C before the particle control device like electrostatic precipitator or fiber filter, it is the zone suitable for injecting powder adsorbents for Hg^0 removal. The deNO_x SCR catalyst was often operated at around 350°C, at which Hg^0 can be oxidized into Hg^{2+} and the downstream wet flue gas desulfurization can successfully remove Hg^{2+}. For the NO removal experiment, the same fixed-bed reactor with 1.0 g sample was used, and the flue gas of 1.5 L min^{-1} contained 6% O_2, 200 ppm NH_3, 200 ppm NO, and balanced N_2 at 150 to 400°C. The test sample was placed in the reactor and heated to 200°C under 500 mL min^{-1} N_2 flow for 1 h to remove the water vapor inside the pore before conducting the removal experiment.

RESULTS AND DISCUSSION

Characterization of Raw and Metal-oxide-incorporated SiO_2

The physical properties of raw and modified rice-husk-derived silica are listed in Table 1. For the raw SiO_2, the S_{BET} was 160 m^2 g^{-1} and V_t was 0.298 cm^3 g^{-1}. The S_{BET} and V_t increased significantly after the incorporation of copper oxide, indicating that the presence of copper oxide did not block or shrink the pore structure of the raw SiO_2; instead, the structure might reconstruct during the hydrothermal synthesis process. Among all the copper-incorporated SiO_2, 50%Cu/SiO_2 demonstrated higher S_{BET} (210 m^2 g^{-1}) and V_t (0.473 cm^3 g^{-1}) than 10% and 25%Cu/SiO_2. Moreover, the S_{BET} was further improved to 260 m^2 g^{-1} after CeO_x addition, indicating that there might be synergistic effects between copper oxides and ceria oxides on building up new structure on the SiO_2 surface. In contrast, 50%Cu-10%Ce/SiO_2 had the lowest V_t (0.278 cm^3 g^{-1}) and the smallest average pore volume (5.2 nm), which might be due to the shrinkage of the original SiO_2 mesopores. This result is consistent with one previous research, in which the CuCeTi catalyst showed higher specific surface area than the CuTi catalyst, suggesting that the introduction of Ce led to highly dispersed copper species on the catalyst surface (Chen *et al.*, 2014).

The X-ray diffraction patterns of raw SiO_2 and metal oxides-incorporated SiO_2 (Fig. 1) showed that no significant peaks corresponding to the crystal phases of SiO_2 were observed among all the test samples, which indicated that the rice-husk-derived silica was amorphous. For 10%Cu/SiO_2 and 25%Cu/SiO_2, only weak diffraction peaks of cubic CuO (2θ = 35.29°, 38.49°) were found (Wang *et al.*, 2013). The diffraction peaks became even weaker as the copper content increased. For 50%Cu/SiO_2, no obvious peak attributed to CuO was detected. This indicated that the copper oxides were amorphous and/or highly dispersed on the surface of SiO_2. Highly dispersed active sites on the surface of the catalyst can result in an enhancement of catalytic activity (Xiang *et al.*, 2015). This result also suggested that there were interactions between copper oxides and SiO_2 and these interactions might lead to more amorphous species formed in SiO_2. Some earlier studies also demonstrated the presence of an amorphous or poorly crystalline state in SCR or mercury removal catalysts (Shu *et al.*, 2012; Li *et al.*, 2012; Xiang *et al.*, 2015; Chi *et al.*, 2017). These amorphous transition metal oxides showed larger Hg^0 catalytic activity than its crystalline phase on the MnO_x-CeO_2/TiO_2 catalyst (Li *et al.*, 2012).

Fig. 2 shows the SEM images of raw and metal-oxide SiO_2, indicating that raw SiO_2 comprised uniform spherical particles with sizes within 0.1–0.15 µm. Changes in surface morphology for SiO_2 were found after the incorporation of metal oxides. The SEM images clearly demonstrated that the particles turned into plate-like structure, confirming that the presence of metal oxides could change the surface morphology of SiO_2 particles. Compared to Fig. 2(b), Fig. 2(c) shows that 50%Cu/SiO_2 had more plate-like particles and the size of the particles was smaller and more uniform. This result can be attributed to its higher copper content. As the copper loading increased, the atomic arrangement of CuO_x/SiO_2 may be closer, which can result in the smaller particle sizes. As shown in Fig. 2(d), the 50%Cu-10%Ce/SiO_2 possessed some layer

Table 1. Physical properties of raw and incorporated rice-husk-derived silica.

Sample	S_{BET} (m^2 g^{-1})	V_t (cm^3 g^{-1})	Average pore size (nm)
Raw SiO_2	160	0.298	6.4
10%Cu/SiO_2	192	0.323	9.0
25%Cu/SiO_2	175	0.408	8.1
50%Cu/SiO_2	210	0.473	6.0
50%Cu-10%Ce/SiO_2	260	0.278	5.2

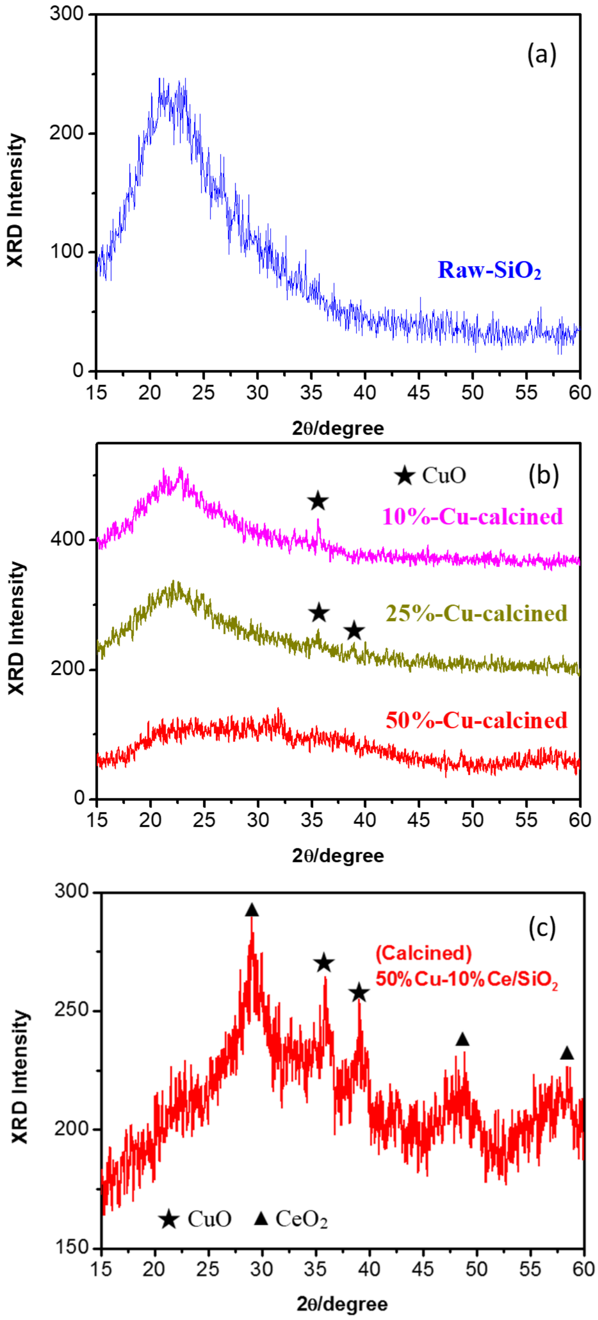

Fig. 1. XRD patterns of (a) raw SiO_2; (b) CuO_x/SiO_2; (c) 50%Cu-10%Ce/SiO_2

structures with many fine metal oxide aggregates attached on them. This result was similar to our previous study (Chiu *et al.*, 2017) that the aggregation and particle growth did not decrease the specific surface area, which indicated that well-structured mesopores were created.

The TEM image of raw SiO_2 (Fig. 3(a)) shows that the typical nanoparticles were well dispersed with the size in the range of 10–15 nm. The porous structure had advantages for dispersion of metal oxides. As the copper content increased, the nanoparticles turned into silk-like with a uniform size and the precipitant of copper oxides started to appear on the SiO_2 surface. The image of 50%Cu-10%Ce/SiO_2 (Fig. 3(d)) shows that great amounts of copper oxide and ceria oxides were present on the surface of SiO_2 and these metal oxides were formed as clusters. This is consistent with the XRD result that uniformed CuO and CeO_x crystallinities were detected on the surface of 50%Cu-10%Ce/SiO_2.

Four samples were further analyzed by XPS in order to investigate the chemical state of species on the surface, and the obtained O1s, Cu2p, and Ce3d spectra are shown in Figs. S2 and S3 and Table 2. The spectra of O1s for the four samples were divided into three single peaks, lattice oxygen at 529.6–530.6 eV (O_α), chemisorbed oxygen at 531.0–532.0 eV (O_β), and oxygen in hydroxyl form and/or surface adsorbed water at 532.0–533.0 eV (O_γ) (Li *et al.*, 2015). Results showed that as the copper content increased, the amount of O_γ decreased and the amount of chemisorbed oxygen increased. Zhang *et al.* (2017) indicated that chemisorbed oxygen played an important role in redox reactions and resulted in enhancing Hg^0 removal efficiency because of its high mobility. In addition, the high ratio of O_β was also helpful for the NO removal efficiency since more NO can be oxidized to NO_2 and enhanced the "fast SCR" reaction: $2NH_3 + NO + NO_2 \rightarrow 2N_2 + H_2O$ (Chi *et al.*, 2017). Although the ratio of chemisorbed oxygen decreased after the addition of ceria oxide, the combination of CuO_x and CeO_x might facilitate the conversion of chemisorbed oxygen and gas-phase O_2 and lead to the high NO removal efficiency (Li *et al.*, 2015).

The Cu2p XPS spectra for the metal oxide-incorporated SiO_2 are shown in Fig. S3. The binding energy peaks at 932.2–932.6 eV could be attributed to Cu^+ while the peaks at 933.2–934.4 eV could be regarded as Cu^{2+} (Chi *et al.*, 2017). The ratio of Cu^{2+} obviously increased as the copper content increased from 10% to 50%; however, the ratio of Cu^{2+} decreased after the addition of ceria oxides. Cu^{2+} was considered to play an important role in NO removal since it can adsorb, activate NO molecules and favor the SCR reaction by the redox cycle between Cu^{2+} and Cu^+ (Yu *et al.*, 2017). Therefore, the higher Cu^{2+} ratio on the 50%Cu/SiO_2 can be a reason for its greater NO removal efficiency.

The deconvolution of XPS core-level O1s, Cu2p, and Ce3d is summarized in Table 2. The results indicated that the relative ratio of Ce^{3+} calculated by $Ce^{3+}/(Ce^{3+} + Ce^{4+})$ on the 50%Cu-10%Ce/SiO_2 was 41.07% and Ce^{4+} was 58.93%. Ceria oxide has great ability to store and release oxygen through the redox shift between Ce^{3+} and Ce^{4+} (Kwon *et al.*, 2015). In addition, Ce^{3+} could create charge imbalance, vacancies, and unsaturated chemical bonds on the surface of catalyts, which could result in more oxygen defects. Therefore, the higher ratio of Ce^{3+} could promote the oxidation of NO to NO_2, thus increasing the NO removal efficiency at low temperature (Shu *et al.*, 2012). 50%Cu-10%Ce/SiO_2 with the high content of Ce^{3+} might provide its best NO removal efficiency among all the samples.

In order to investigate the redox property of the metal oxide-incorporated SiO_2, H_2-TPR was conducted and shown in Fig. S4. For 10, 25, and 50%Cu/SiO_2, two different peaks were found. The low temperature peak at around 225°C could be attributed to the reduction of isolated $Cu^{2+} \rightarrow Cu^+$, while the high temperature peak at around 325°C could be

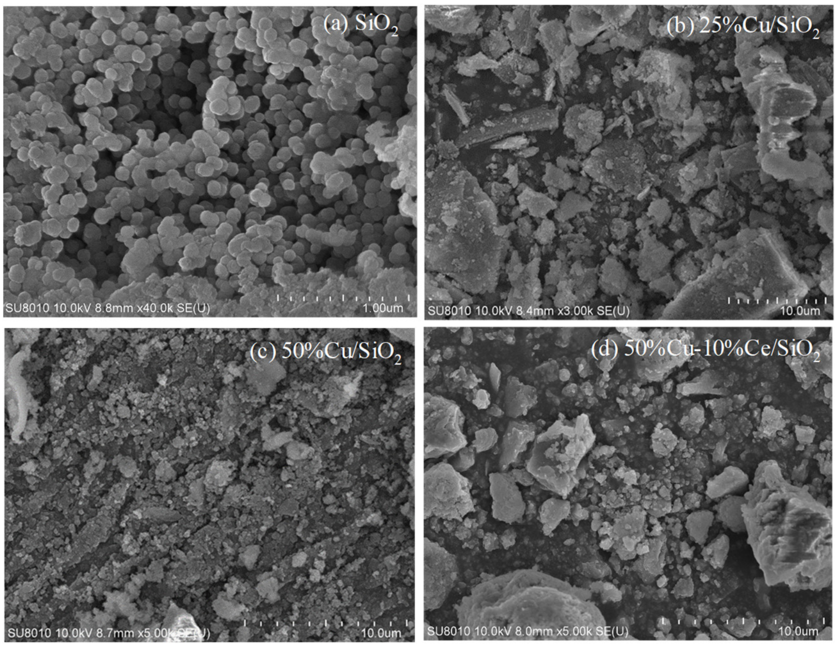

Fig. 2. SEM images of metal oxide-incorporated SiO_2.

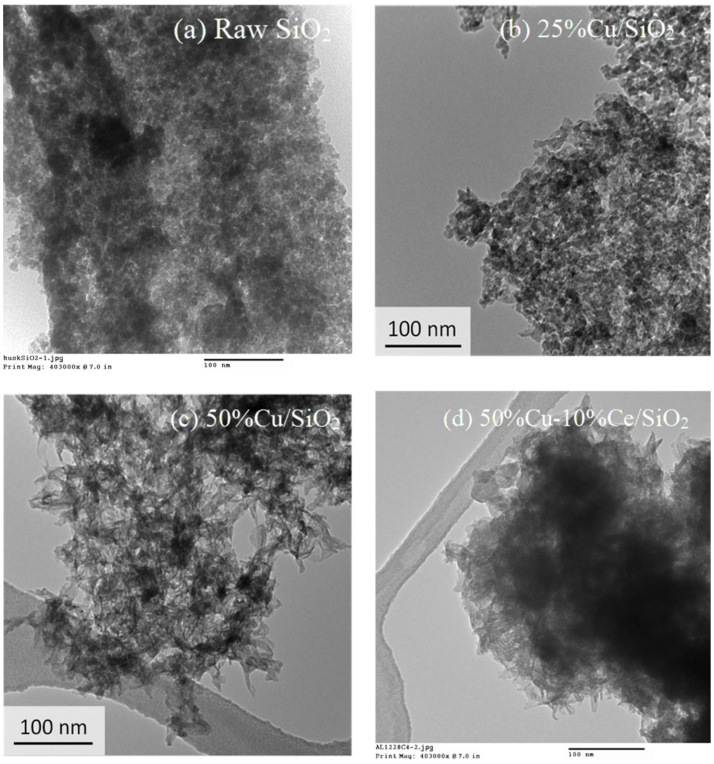

Fig. 3. TEM images of raw and metal oxide-incorporated SiO_2.

Table 2. XPS results of metal oxide-incorporated SiO_2.

Sample	Peak area (%)						
	O_α	O_β	O_γ	Cu^+	Cu^{2+}	Ce^{3+}	Ce^{4+}
10%Cu/SiO_2	17.66	33.95	48.39	40.64	59.36	-	-
25%Cu/SiO_2	22.12	35.32	42.56	31.99	68.01	-	-
50%Cu/SiO_2	23.51	57.87	18.62	15.46	84.54	-	-
50%Cu-10%Ce/SiO_2	58.18	41.82	-	45.4	54.6	41.07	58.93

regarded as the the reduction of CuO to Cu^0 (Niu *et al.*, 2016). After the addition of ceria oxide, the peak at higher temperature disappeared, and one large peak at about 266°C was observed. This result suggested that the interaction between copper and ceria oxides might lead to an easier reduction of ceria and CuO (Mrabet *et al.*, 2012).

NH_3-TPD was carried out to further investigate the acid sites on the metal oxide-incorporated SiO_2. The results are shown in Fig. S5. All the samples had a broad peak that started at 150°C and ended at around 450°C, which could be regarded as ammonia desorbed from Brönsted acid sites (Pan *et al.*, 2014), and the peak of 50%Cu/SiO_2 at higher temperature (about 600 to 700°C) could be assigned to the NH_3 desorbed from Lewis acid sites (Boxiong *et al.*, 2014). Since Lewis acid sites are the primary acid sites evolved at high temperatures, the great amount of Lewis acid sites on 50%Cu/SiO_2 might improve the NO removal efficiency at higher temperature. The peak area of the 50%Cu/SiO_2 and 50%Cu-10%Ce/SiO_2 was much larger than that of the other two samples. Because the quanity of NH_3 is proportional to the surface acid amount, this result could be concluded as that the 50%Cu/SiO_2 and 50%Cu-10%Ce/SiO_2 samples had stronger acidity. These results were also consistent with the H_2-TPR results and might lead to the better catalytic activity of 50%Cu/SiO_2 and 50%Cu-10%Ce/SiO_2.

NO Removal Efficiency of Metal-oxide SiO_2

NO Removal of Metal-oxide SiO_2 at Various metal Components and Temperature

Fig. 4 clearly shows that the raw SiO_2 did not demonstrate any NO removal efficiency from 200 to 300°C and the removal efficiency became negative with further increase in temperature, which was mainly due to the direct reaction of NH_3 with O_2 to form nitrogen oxides (Piubello *et al.*, 2016). In contrast, the NO removal efficiency of CuO_x/SiO_2 first increased with the increasing temperatures and then decreased when temperature was higher than 300°C, which might also be due to the NH_3 oxidation at high temperature. Similar test results can be found in previous research that the NO conversion efficiency of 8%Cu/SCR catalyst started to decrease when the temperature was above 300°C (Chi *et al.*, 2017).

The NO removal efficiency also increased as the copper content increased. 25%Cu/SiO_2 exhibited similar NO removal efficiency with 10%Cu/SiO_2 at temperature below 300°C but became greater at higher temperature. 50%Cu/SiO_2 showed a significant improvement in NO removal efficiency at all test temperatures, which might relate to its largest S_{BET} and a greater amount of Cu^{2+} and surface chemisorbed oxygen.

The influence of CeO_x modification on the improvement of NO removal efficiency for CuO_x/SiO_2 was also investigated. The addition of ceria oxides successfully improved the NO removal efficiency at low temperature. 50%Cu-10%Ce/SiO_2 showed the best NO conversion efficiency of 70–85% and a broad temperature window of 150–300°C. This result can be attributed to its large S_{BET} (i.e., 260 $m^2\ g^{-1}$) and great amount of Ce^{3+} (Table 2) that can create charge imbalance, vacancies, and unsaturated chemical bonds on the catalyst surface (Li *et al.*, 2015), thus increasing the ability to adsorb, store, and transfer the surface oxygen and further enhancing the deNO activity at low temperature (Sohot *et al.*, 2012). Li *et al.* (2015) also showed that the NO reduction efficiency of CuCeTi catalysts was significantly higher than that of CuTi and CeTi catalysts in low-temperature range (150–250°C), which was similar to our test results. Because 50%Cu/SiO_2 and 50%Cu-10%Ce/SiO_2 had the superior NO removal efficiency among all the test samples, these two samples were futher investigated under different flue gas conditions.

Effect of H_2O and SO_2 on NO Removal

To clarify the influence of H_2O on the NO removal test over 50%Cu/SiO_2 and 50%Cu-10%Ce/SiO_2, 10% H_2O was initially injected into the gas mixing chamber and then stopped injection after 2 h. Fig. 5(a) shows the effect of H_2O on deNO$_x$ efficiency of the samples at 250°C. The NO removal efficiency of 50%Cu/SiO_2 rapidly decreased to about 28% after the addition of H_2O, but the deactivation was reversible since the removal efficiency recovered to its

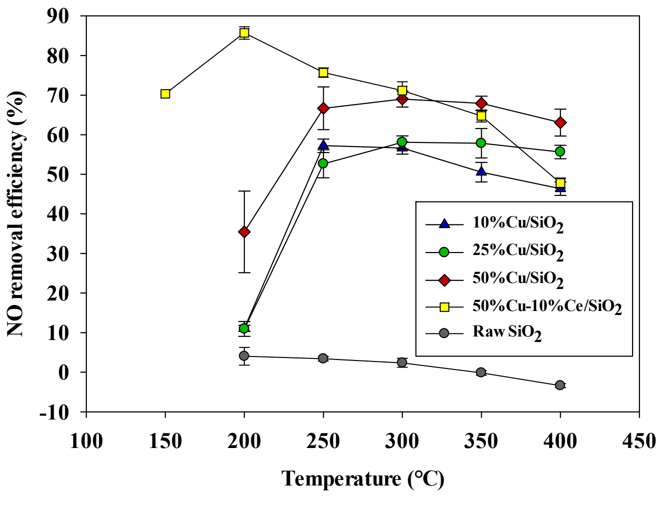

Fig. 4. Effect of temperature on NO removal efficiency of different samples. The flue gas condition is NO: 200 ppm; NH_3: 200 ppm; O_2: 6%; space velocity: 3600 h^{-1}.

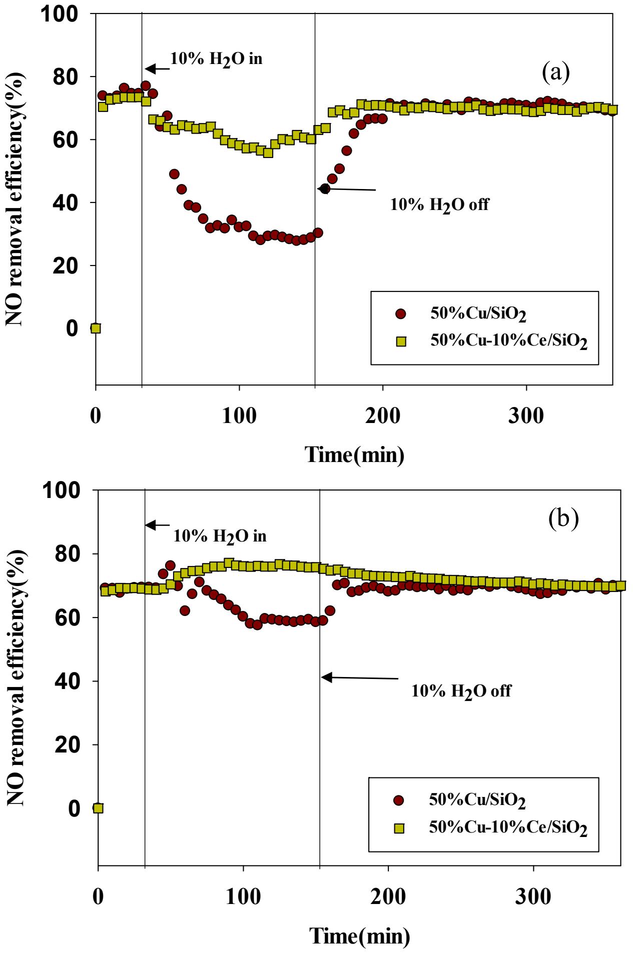

Fig. 5. Effect of H_2O on NO removal efficiency at (a) 250°C and (b) 300°C. The flue gas condition is NO: 200 ppm; NH_3: 200 ppm; O_2: 6%; H_2O: 10% (within first 2 h) space velocity: 3600 h^{-1}.

original level after stopped injecting H_2O. In contrast, the deactivation caused by H_2O was less obvious for the 50%Cu-10%Ce/SiO_2 sample, which might be due to its larger S_{BET}. This phenomenon has been found in several studies showing that H_2O has a reversible negative effect on the NO conversion efficiency at lower temperature (Du *et al.*, 2013; Pan *et al.*, 2013). The inhibition effect by H_2O can be attributed to competitive adsorption between H_2O and NH_3 on the active sites (Pan *et al.*, 2013).

The effect of H_2O at 300°C is shown in Fig. 5(b). The inhibition caused by H_2O became less significant as the temperature increased to 300°C. Moreover, the addition of H_2O showed a promotion on NO removal over 50%Cu-10%Ce/SiO_2 at 300°C, and the NO removal efficiency slightly decreased after H_2O was removed. This result is similar to previous research that the NO conversion over Ce-based catalyst was improved after the introduction of H_2O at higher temperature and the promotional effect could be attributed to the inhibition of NH_3 oxidation (Du *et al.*, 2013; Xiao *et al.*, 2016).

Fig. 6 shows the effect of SO_2 on the NO removal efficiency of 50%Cu/SiO_2 and 50%Cu-10%Ce/SiO_2 at 250 and 300°C. 200 ppm of SO_2 was injected into the gas mixing chamber for 900 min under this condition. The NO removal efficiency was calculated after the 15 h test. As shown in Fig. 6(a), the NO removal efficiency of both two samples significantly decreased after the injection of SO_2 at 250°C. The NO reduction activity of 50%Cu/SiO_2 decreased from 70.7% to 24.6%. 50%Cu-10%Ce/SiO_2 showed a better SO_2 resistance since the NO removal efficiency decreased from 77.9% to 42.1% after the addition of SO_2 at 250°C. The reduction in NO removal efficiency at low temperature might cause by the formation of ammonia sulfate or sulfite salts such as $(NH_4)_2SO_3$, $(NH_4)_2SO_4$, and NH_4HSO_4. These species could deposit on the surface of the samples and blocked the active sites, thus restrained NO and NH_3 adsorption and further decreased the SCR activity (Ma *et al.*, 2013). Xie *et al.* (2004) also indicated that the formation of $CuSO_4$ during the reaction could deactivated the catalyst by either pore filling and/or plugging or by its low NO removal efficiency compared to the CuO. The role of ceria on SO_2 resistance

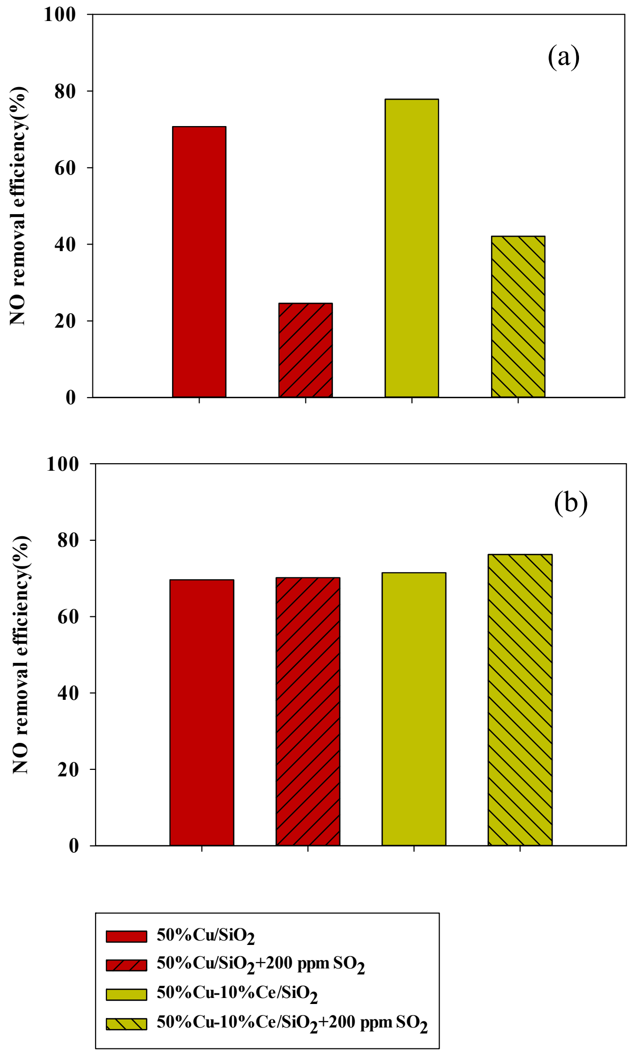

Fig. 6. Effect of SO_2 on NO removal efficiency at (a) 250°C and (b) 300°C. The flue gas condition is NO: 200 ppm; NH_3: 200 ppm; O_2: 6%; SO_2: 200 ppm (when need) space velocity: 3600 h^{-1}.

has also been investigated. Kwon *et al.* (2015) indicated that the V/Sb/Ce/Ti catalyst showed an excellent SO_2 resistance compared to V/Sb/Ti catalyst since the formation of NH_4HSO_4 over the V/Sb/Ce/Ti catalyst could be inhibited by consuming SO_2 in the formation of $Ce_2(SO_4)_3$.

Fig. 6(b) shows the effect of SO_2 on NO removal efficiency at 300°C. The results revealed that the NO reduction activity over 50%Cu/SiO_2 almost remained constant after the injection of 200 ppm SO_2. The addition of 200 ppm SO_2 even led to a promotion effect over 50%Cu-10%Ce/SiO_2 at 300°C since the NO removal efficiency slightly increased from 71.5% to 76.3%. Xie *et al.* (2004) indicated that ammonia sulfate salt such as $(NH_4)_2SO_4$ and NH_4HSO_4, which were considered to be the deactivating agents for SCR catalysts at low temperatures, would decompose at temperatures of 250–450°C. Xiao *et al.* (2016) also showed that the introduction of SO_2 caused a promotion effect of NO reduction over the Ce/TiO_2 catalyst at higher temperature, and the promotion could be attributed to the sulfation of catalyst. The Ce/TiO_2 catalyst demostrated a great NH_3 adsorption ability and the the catalytic oxidation of NH_3 to NO was inhibited after the sulfation at high temperature.

Hg Removal Test

Hg Removal Efficiency of Various Metal-oxide SiO_2

The total Hg (T-Hg) removal efficiency was tested with Cu/SiO_2 and 50%Cu-10%Ce/SiO_2. The results indicated that none of these four samples reached adsorption equilibrium during the test duration of 900 min, indicating that the adsorption did not obtain complete breakthrough. Fig. 7(a) shows that 50%Cu/SiO_2 had a higher average T-Hg removal efficiency (88.2%) than 10%Cu/SiO_2 (85.3%) and 25%Cu/SiO_2 (82.5%). This test result is expected since 50%Cu/SiO_2 had the largest S_{BET} and the greatest amount of CuO_x highly dispersed on the surface. Furthermore, the high ratio of Cu^{2+} and chemisorbed oxygen can also lead to its greatest mercury removal efficiency. This result is similar to our previous research that a very large amount (approximately 50%) of CuO_x was introduced into mesoporous SiO_2 and presented an excellent performance for Hg^0 removal under the flue gas condition (Chiu *et al.*, 2017).

Fig. 7(b) shows that the T-Hg removal efficiencies of 50%Cu/SiO_2 and 50%Cu-10%Ce/SiO_2 were almost the same during the first 400 min. However, the T-Hg removal efficiency of 50%Cu-10%Ce/SiO_2 slightly decreased to about 55% at the end of the Hg^0 removal test. This result indicated that the modification of CeO_x did not enhance the T-Hg removal efficiency and the durability of the sample was also decreased. Although 50%Cu-10%Ce/SiO_2 had the largest specific surface area, the CuO and CeO_x crystallinity and the lower ratio of Cu^{2+} and surface chemisorbed oxygen might be the reason for its poor durability.

Effect of Inlet Hg^0 Concentration and Temperature on Hg Removal Efficiency of Metal-oxide SiO_2

Table 3 shows that 50%Cu/SiO_2 had great T-Hg removal efficiency when the inlet Hg^0 concentration increased to 65 µg m^{-3}. However, the average removal efficiency decreased to 63.1% at 100 µg m^{-3} inlet Hg^0 concentration. The corresponding adsorption capacity was 3330.6, 7769.9, and 8989.2 µg g^{-1} at 30, 65, and 100 µg m^{-3} Hg^0, respectively.

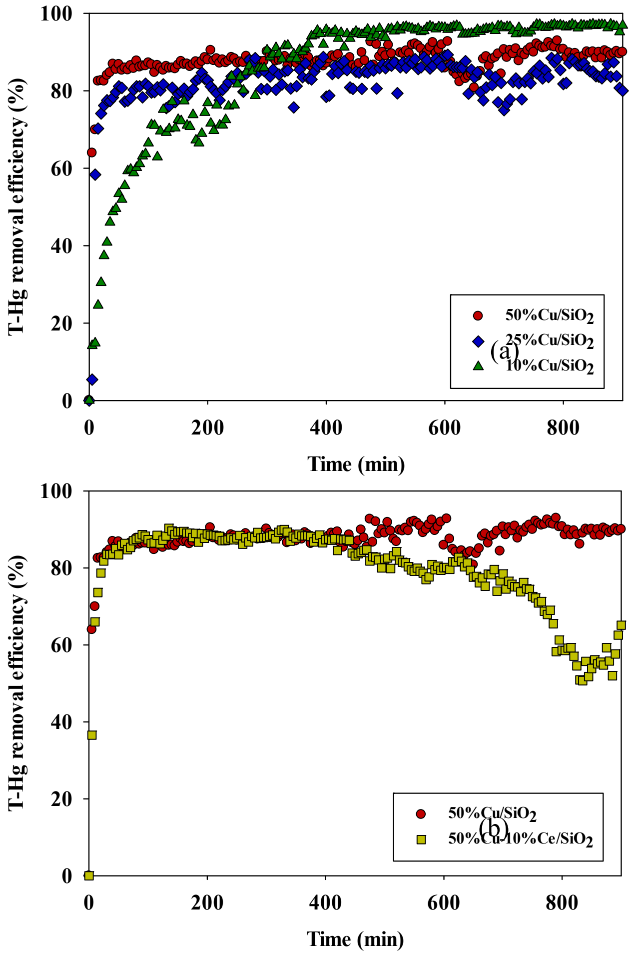

Fig. 7. T-Hg removal efficiency of (a) Cu/SiO_2 samples and (b) 50%Cu/SiO_2 and 50%Cu-10%Ce/SiO_2 for comparison. The flue gas condition is Hg^0: 30 µg m^{-3}; NO: 200 ppm; SO_2: 200 ppm; HCl: 50 ppm; H_2O: 10%; CO_2: 12%; O_2: 6%; temperature: 150°C; space velocity: 120000 hr^{-1}.

Table 4 shows that the T-Hg removal efficiency for 50%Cu/SiO_2 remained almost the same as the temperature increased from 150 to 250°C. When the temperature increased to 350°C, the removal efficiency decreased to 55.3%. Futhermore, the Hg adsorption capacity was 3330.6, 3421.5, 2524.4 µg g^{-1} at 150, 250, and 350°C, respectively. These results indicated that the 50%Cu/SiO_2 still possessed an excellent adsorption performance even when temperature increased to 250°C, and the decrease of T-Hg removal efficiency at 350°C was expected since the adsorption of Hg was thermodynamically unfavorable at higher temperature (Chiu *et al.*, 2015).

CONCLUSIONS

This study investigated the effects of metal oxide incorporation with rice-husk-derived silica on the physicochemical properties and NO/Hg removal efficiency of CuO_x- and CuO_x-CeO_x/SiO_2 from simulated flue gases.

Table 3. T-Hg removal of 50%Cu/SiO_2 under various inlet Hg^0 concentration.

Inlet Hg^0 concentration ($\mu g\ m^{-3}$)	Temperature (150°C)		
	Adsorption time (min)	Hg adsorption capacity ($\mu g\ g^{-1}$)	Avg. T-Hg removal (%)
30	900	3330.6	88.2
65	900	7769.9	90.2
100	900	8989.2	63.1

Table 4. T-Hg removal of 50%Cu/SiO_2 under various temperatures.

Temperature (°C)	Inlet Hg^0 concentration (30 $\mu g\ m^{-3}$)		
	Adsorption time (min)	Hg adsorption capacity ($\mu g\ g^{-1}$)	Avg. T-Hg removal (%)
150	900	3330.6	88.2%
250	900	3421.5	89.3%
350	900	2524.4	55.3%

The goal was to develop a new SCR catalyst and Hg adsorbent from two wastes: copper-containing wastewater and rice-husk-derived silica, and to understand the effects of flue gas conditions on removal of Hg^0 and NO. The primary conclusions are summarized as below:

(1) The specific surface area of rice-husk-derived SiO_2 significantly increased after the surface modification by metal oxides. XPS results showed that Cu^{2+} and Ce^{4+} were the major valence states presenting in metal-oxide SiO_2. H_2-TPR and NH_3-TPD indicated that 50%Cu/SiO_2 and 50%Cu-10%Ce/SiO_2 had better redox ability and stronger acidity.

(2) The incorporation of Cu and Ce oxides successfully improved the NO removal efficiency. 50%Cu-10%Ce/SiO_2 showed the best NO removal efficiency and a broad temperature window, which may be due to its highest specific area and great redox ability and acidity.

(3) 50%Cu/SiO_2 exhibited greatest T-Hg removal efficiency among all the tested samples under flue gas condition at 150°C, which may be due to its large specific surface area and great amount of CuO_x highly dispersed on the surface.

(4) Rice-husk-derived SiO_2 incorporated with copper ion recycled from industrial wastewater has been shown successfully fabricated via silicate-exfoliation hydrothermal processes and is verified with good removal effectiveness for both Hg^0 and NO. As noted earlier, because the SiO_2 support and Cu ion are both recycled from agricultural and industrial wastes, the resulting products can be considered as environment-friendly catalysts and adsorbents.

ACKNOWLEDGMENTS

This study was financially supported by the Ministry of Science and Technology of Taiwan (MOST 103-2622-E-002-038-CC3).

NOTES

The authors declare no competing financial interest.

SUPPLEMENTARY MATERIAL

Supplementary data associated with this article can be found in the online version at http://www.aaqr.org.

REFERENCES

Adam, F., Appaturi, J.N. and Iqbal, A. (2012). The utilization of rice husk silica as a catalyst: Review and recent progress. *Catal. Today* 190: 2–14.

Boxiong, S., Hongqing, M., Chuan, H. and Xiaopeng, Z. (2014). Low temperature NH_3-SCR over Zr and Ce pillared clay based catalysts. *Fuel Proc. Technol.* 119: 121–129.

Chang, H., Wu, Q., Zhang, T., Li, M., Sun, X., Li, J., Duan, L. and Hao, J. (2015). Design strategies for CeO_2-MoO_3 catalysts for $deNO_x$ and Hg^0 oxidation in the presence of HCl: The significance of the surface acid-base properties. *Environ. Sci. Technol.* 49: 12388–12394.

Chen, L., Si, Z., Wu, X. and Weng, D. (2014). DRIFT study of CuO-CeO_2-TiO_2 mixed oxides for NO_x reduction with NH_3 at low temperatures. *ACS Appl. Mater. Interfaces* 6: 8134–8145.

Chen, Y., Wang, M., Du, X., Ran, J., Zhang, L. and Tang, D. (2018). High resistance to Na poisoning of the V_2O_5-$Ce(SO_4)_2$/TiO_2 catalyst for the NO SCR reaction. *Aerosol Air Qual. Res.* 18: 2948–2955.

Chi, G.L., Shen, B.X., Yu, R.R., He, C. and Zhang, X. (2017). Simultaneous removal of NO and Hg^0 over Ce-Cu modified V_2O_5/TiO_2 based commercial SCR catalysts. *J. Hazard. Mater.* 330: 83–92.

Chiu, C.H., Hsi, H.C. and Lin, H.P. (2015). Multipollutant control of Hg/SO_2/NO from coal-combustion flue gases using transition metal oxide-impregnated SCR catalysts. *Catal. Today* 245: 2–9.

Chiu, C.H., Kuo, T.H., Chang, T.C., Lin, S.F., Lin, H.P. and Hsi, H.C. (2017). Multipollutant removal of Hg^0/SO_2/NO from simulated coal-combustion flue gases using metal oxide/mesoporous SiO_2 composites. *Int. J. Coal Geol.* 170: 60–68.

Chou, C.P., Chang, T.C., Chiu, C.H. and Hsi, H.C. (2018). Mercury speciation and mass distribution in cement production process of Taiwan. *Aerosol Air Qual. Res.* 18:

2801–2812.

Deng, M., Zhang, G., Peng, X., Lin, J., Pei, X. and Huang, R. (2016). A facile procedure for the synthesis of δ-$Na_2Si_2O_5$ using rice husk ash as silicon source. *Mater. Lett.* 163: 36–38.

Du, X., Gao, X., Cui, L., Zheng, Z., Ji, P., Luo, Z. and Cen, K. (2013). Experimental and theoretical studies on the influence of water vapor on the performance of a Ce-Cu-Ti oxide SCR catalyst. *Appl. Surf. Sci.* 270: 370–376.

Fan, Y., Ling, W., Dong, L., Li, S., Yu, C., Huan, B. and Xi, H. (2018). In situ FT-IR and DFT study of the synergistic effects of cerium presence in the framework and the surface in NH_3-SCR. *Aerosol Air Qual. Res.* 18: 655–670.

Gao, J., Yue, T., Zuo, P., Liu, Y., Tong, L., Wang, C., Zhang, X. and Qi, S. (2017) Current status and atmospheric mercury emissions associated with large-scale gold smelting industry in China. *Aerosol Air Qual. Res.* 17: 238–244.

Gao, X., Du, X., Cui, L., Fu, Y., Luo, Z. and Cen, K. (2010). A Ce-Cu-Ti oxide catalyst for the selective catalytic reduction of NO with NH_3. *Catal. Commun.* 12: 255–258.

He, J., Reddy, G.K., Thiel, S.W., Smirniotis, P.G. and Pinto, N.G. (2013). Simultaneous removal of elemental mercury and NO from flue gas using CeO_2 modified MnO_x/TiO_2 materials. *Energy Fuels* 27: 4832–4839.

Jiang, Y., Bao, C., Liu, S., Liang, G., Lu, M., Lai, C., Shi, W. and Ma, S. (2018). Enhanced activity of Nb-modified CeO_2/TiO_2 catalyst for the selective catalytic reduction of NO with NH_3. *Aerosol Air Qual. Res.* 18: 2121–2130.

Kwon, D.W., Nam, K.B. and Hong, S.C. (2015). The role of ceria on the activity and SO_2 resistance of catalysts for the selective catalytic reduction of NO_x by NH_3. *Appl. Catal. B Environ.* 166: 37–44.

Li, H.,Wu, C.Y., Li, Y. and Zhang, J. (2012). Superior activity of MnO_x-CeO_2/TiO_2 catalyst for catalytic oxidation of elementalmercury at low flue gas temperatures. *Appl. Catal., B* 111–112: 381–388.

Li, H.L., Li, Y., Wu, C.Y. and Zhang, J.Y. (2011). Oxidation and capture of elemental mercury over SiO_2-TiO_2-V_2O_5 catalysts in simulated low-rank coal combustion flue gas. *Chem. Eng. J.* 169: 186–193.

Li, H.L., Wu, S.K., Li, L.Q., Wang, J., Ma, W.W. and Shih, K.M. (2015). CuO-CeO_2/TiO_2 catalyst for simultaneous NO reduction and Hg^0 oxidation at low temperatures. *Catal. Sci. Technol.* 5: 5129–5138.

Lin, C.J., Chang, C.L., Tseng, C.F., Lin, H.P. and Hsi, H.C. (2019) Preparation of Cu-Mn and Cu-Mn-Ce oxide/mesoporous silica via silicate exfoliation for removal of NO and Hg^0. *Aerosol Air Qual. Res.* 19: 1421–1438.

Liu, C., Chen, L., Li, J., Ma, L., Arandiyan, H., Du, Y., Xu, J. and Hao, J. (2012). Enhancement of activity and sulfur resistance of CeO_2 supported on TiO_2-SiO_2 for the selective catalytic reduction of NO by NH_3. *Environ. Sci. Technol.* 46: 6182–6189.

Liu, K.H., Chen, M.Y., Tsai, Y.C., Lin, H.P. and Hsi, H.C. (2017). Control of Hg^0 and NO from coal-combustion flue gases using MnO_x-CeO_x/mesoporous SiO_2 from waste rice husk. *Catal. Today* 297: 104–112.

Liu, L., Zheng, C., Wang, J., Zhang, Y., Gao, X. and Cen, K. (2018). NO adsorption and oxidation on Mn doped CeO_2 (111) surfaces: A DFT+U study. *Aerosol Air Qual. Res.* 18: 1080–1088.

Ma, Z., Yang, H., Li, B., Liu, F. and Zhang, X. (2013). Temperature-dependent effects of SO_2 on selective catalytic reduction of NO over Fe-Cu-O_x/CNTs-TiO_2 catalysts. *Ind. Eng. Chem. Res.* 52*:* 3708–3713.

Mrabet, D., Abassi, A., Cherizol, R. and Do, T.O. (2012). One-pot solvothermal synthesis of mixed Cu-Ce-O_x nanocatalysts and their catalytic activity for low temperature CO oxidation. *Appl. Catal., A* 447–448: 60–66.

Niu, C., Shi, X., Liu, F., Liu, K., Xie, L., You, Y. and He, H. (2016). High hydrothermal stability of Cu-SAPO-34 catalysts for the NH_3-SCR of NO_x. *Chem. Eng. J.* 294: 254–263.

Pan, S., Luo, H., Li, L., Wei, Z. and Huang, B. (2013). H_2O and SO_2 deactivation mechanism of MnO_x/MWCNTs for low-temperature SCR of NO_x with NH_3. *J. Mol. Catal. A: Chem.* 377: 154–161.

Pan, W.G., Zhou, Y., Guo, R.T., Zhen, W.L., Hong, J.N., Xu, H.J., Jin, Q., Ding, C.G. and Guo, S.Y. (2014). Influence of calcination temperature on CeO_2-CuO catalyst for the selective catalytic reduction of NO with NH_3. *Environ. Prog. Sustainable Energy* 33: 385–389.

Peng, Y., Liu, C.X., Zhang, X.Y. and Li, J.H. (2013). The effect of SiO_2 on a novel CeO_2-WO_3/TiO_2 catalyst for the selective catalytic reduction of NO with NH_3. *Appl. Catal., B* 140–141: 276–282.

Piubello, F., Jangjou, Y., Nova, I. and Epling, W.S. (2016). Study of NO formation during NH_3 oxidation reaction over a Cu-SAPO-34 SCR catalyst. *Catal. Lett.* 146: 1552–1561.

Shu, Y., Sun, H., Quan, X. and Chen, S. (2012). Enhancement of catalytic activity over the iron-modified Ce/TiO_2 catalyst for selective catalytic reduction of NO_x with ammonia. *J. Phys. Chem. C* 116: 25319–25327.

Sohot, M.R., Jasis, U.S. and Sulaiman, M.R. (2012). IEEE Symposium on Business Engineering and Industrial Applications (ISBEIA), doi: 10.1109/ISBEIA.2012.6422999.

Song, H., Zhang, M., Yu, J., Wu, W., Qu, R., Zheng, C. and Gao, X. (2018). The effect of Cr addition on Hg^0 oxidation and NO reduction over V_2O_5/TiO_2 catalyst. *Aerosol Air Qual. Res.* 18: 803–810.

Sullivan, J.A. and Doherty, J.A. (2005). NH_3 and urea in the selective catalytic reduction of NO_x over oxide-supported copper catalysts. *Appl. Catal., B* 55: 185–194.

Tan, Z., Su, S., Qiu, J., Kong, F., Wang, Z., Hao, F. and Xiang, J. (2012). Preparation and characterization of Fe_2O_3-SiO_2 composite and its effect on elemental mercury removal. *Chem. Eng. J.* 195–196: 218–225.

UNEP (2018). Global Mercury Assessment 2018. UN Environment Programme, Chemicals and Health Branch Geneva, Switzerland.

U.S. EPA. (2019). Air Pollutant Emissions Trends Data. https://www.epa.gov/air-emissions-inventories/air-pollutant-emissions-trends-data, Last Access: January 2019.

Wang, P.Y., Su, S., Xiang, J., Cao, F., Sun, L.S., Hu, S. and Lei, S.Y. (2013). Catalytic oxidation of Hg^0 by CuO-

MnO_2-Fe_2O_3/γ-Al_2O_3 catalyst. *Chem. Eng. J.* 225: 68–75.
Wang, P.Y., Su, S., Xiang, J., You, H., Cao, F., Sun, L., Hu, S. and Zhang, Y. (2014). Catalytic oxidation of Hg^0 by MnO_x-CeO_2/γ-Al_2O_3 catalyst at low temperatures. *Chemosphere* 101: 19–54.
Xiang, J., Wang, P., Su, S., Zhang, L., Cao, F., Sun, Z., Xiao, X., Sun, L. and Hu, S. (2015). Control of NO and Hg^0 emissions by SCR catalysts from coal-fired boiler. *Fuel Process. Technol.* 135: 168–173.
Xiao, X., Xiong, S., Shi, Y., Shan, W. and Yang. S. (2016). Effect of H_2O and SO_2 on the selective catalytic reduction of NO with NH_3 over Ce/TiO_2 catalyst: Mechanism and kinetic study. *J. Phys. Chem. C* 120: 1066–1076.
Xie, G., Liu, Z., Zhu, Z., Liu, Q., Ge, J. and Huang, Z. (2004). Simultaneous removal of SO_2 and NO_x from flue gas using a CuO/Al_2O_3 catalyst sorbent II. promotion of SCR activity by SO_2 at high temperatures. *J. Catal.* 224: 42–49.
Xiong, S.C., Xiao, X., Huang, N., Dang, H., Liao, Y., Zou, S.J. and Yang, S.J. (2017). Elemental mercury oxidation over Fe-Ti-Mn spinel: Performance, mechanism, and reaction kinetics. *Environ. Sci. Technol.* 51: 531–539.
Yalçin, N. and Sevinç, V. (2001). Studies on silica obtained from rice husk. *Ceram. Int.* 27: 219–224.
Yu, X.N., Cao, F.F., Zhu, X.B., Zhu, X.C., Gao, X., Luo, Z.Y. and Cen, K.F. (2017). Selective catalytic reduction of NO over Cu-Mn/OMC catalysts: Effect of preparation method. *Aerosol Air Qual. Res.* 17: 302–313.
Zhang, J., Li, C., Zhao, L., Wang, T., Li, S. and Zeng, G. (2017). A sol-gel Ti-Al-Ce-nanoparticle catalyst for simultaneous removal of NO and Hg^0 from simulated flue gas. *Chem. Eng. J.* 313: 1535–1547.
Zhao, L.K., Li, C.T., Li, S.H., Wang, Y., Zhang, J.Y., Wang, T. and Zeng, G.M. (2016). Simultaneous removal of elemental mercury and NO in simulated flue gas over V_2O_5/ZrO_2-CeO_2 catalyst. *Appl. Catal., B* 198: 420–430.
Zhao, S.J., Ma, Y.P., Qu, Z., Yan, N.Q., Li, Z., Xie, J.K. and Chen, W.M. (2014). The performance of Ag doped V_2O_5-TiO_2 catalyst on the catalytic oxidation of gaseous elemental mercury. *Catal. Sci. Technol.* 4: 4036–4044.

Received for review, September 21, 2019
Revised, October 14, 2019
Accepted, October 19, 2019